Efficient Sensitivity Analysis of Lossy Multiconductor Transmission Lines With Nonlinear Terminations

Anestis Dounavis, Ramachandra Achar, *Member, IEEE*, and Michel S. Nakhla, *Fellow, IEEE*

***Abstract*—An efficient approach for sensitivity analysis of lossy multiconductor transmission lines in the presence of nonlinear terminations is described. Sensitivity information is extracted using the recently developed closed-form matrix-rational approximation of distributed transmission-line model. The method enables sensitivity analysis of interconnect structures with respect to both electrical and physical parameters. An important advantage of the proposed approach is that the derivatives of the modified nodal admittance matrices with respect to per-unit-length parameters are obtained analytically.**

***Index Terms*—Interconnects, optimization, sensitivity analysis, transmission lines.**

I. Introduction

THE ever-increasing quest for higher operating speeds, miniature devices, and denser layouts has made signal integrity analysis a challenging task. As signal frequencies approach the gigahertz range, interconnects behave like distributed transmission lines and effects such as signal delay, crosstalk, ringing, and distortion become prominent. This phenomenon can be observed at many levels of hierarchy, such as on-chip, packaging, multichip modules (MCMs), and printed circuit boards (PCBs). Consequently, improperly designed interconnects can result in poor performance, reliability and may cause false switching [1]–[4].

Interconnects play an important role in determining the circuit's density, power consumption, and clock frequency. For example, increasing the circuit's density leads to shorter interconnects which reduce the problem of delay and reflections. However, this leads to greater crosstalk between adjacent interconnects. Designers must make proper tradeoffs, often between conflicting design requirements, to obtain the best possible performance. Hence, efficient and accurate sensitivity information with respect to interconnect parameters are required by optimizers to solve large nonlinear circuits with embedded distributed subnetworks [5]–[7].

However, for large nonlinear networks with distributed interconnects, the task of finding the best possible design becomes too complicated due to the following difficulties.

1) The first major difficulty is due to the mixed frequency/time problem, which is encountered while linking distributed transmission lines with nonlinear circuit simulators. This is because, distributed transmission lines are described by partial differential equations which are best solved in the frequency domain, whereas nonlinear elements are described only in the time domain (nonlinear ordinary differential equations). Hence, it is essential to model interconnects such that they can be directly included in a nonlinear circuit simulation environment.
2) The second difficulty is due to the excessive CPU time associated with the simulation of interconnect networks.

A significant amount of research has been done to address the simulation of distributed interconnects in the presence of nonlinear elements [1]–[17]. Approaches based on conventional lumped segmentation provide a brute force solution to the mixed frequency/time problem [8]. However, this leads to large circuit matrices, rendering the simulation inefficient. Also, there exist other algorithms based on the method of characteristics [9], [10], optimization techniques [11], Chebyshev polynomials [7], [12], and integral congruent transformations [13]. Recently, an efficient multiconductor transmission-line (MTL) model based on a closed-form Padé approximation has been proposed [14]–[16]. The advantages of this algorithm are as follows: the macromodel of the transmission-line equations is obtained analytically (in terms of predetermined constants and the per-unit-length parameters), the passivity of the macromodel is guaranteed, the method can be easily incorporated with passive model-reduction algorithms [16], [17], and the method can handle transmission lines with lossy as well as frequency-dependent parameters.

In this paper, a new method to perform sensitivity analysis of nonlinear circuits with distributed transmission lines is presented. The method uses a matrix-rational approximation-based algorithm to model distributed interconnects as well as to derive the network sensitivity with respect to any interconnect parameter. A major advantage of the proposed method is that the derivatives of the circuit matrices are obtained analytically, in terms of predetermined constants and per-unit-length parameters, facilitating efficient formulation of the sensitivity network.

The rest of the paper is organized as follows. In Section II, a brief review of formulation of circuit equations is given. In Section III, we outline the steps involved in the sensitivity analysis. Section IV presents the proposed algorithm for sensitivity analysis of nonlinear networks with distributed components. In Sections V and VI, we present the computational results and conclusions, respectively.

II. Formulation of Circuit Equations

In general, distributed networks in the presence of nonlinear elements can be expressed as

$$\begin{aligned} &\boldsymbol{C}_\phi \dot{\boldsymbol{x}}_\phi(t) + \boldsymbol{G}_\phi \boldsymbol{x}_\phi(t) + \sum_{k=1}^{N_t} \boldsymbol{D}_{\boldsymbol{k}} \boldsymbol{i}_{\boldsymbol{k}}(t) + \boldsymbol{f}_\phi\big(\boldsymbol{x}_\phi(t)\big) \\ &\quad = \boldsymbol{b}_\phi(t) \\ &\boldsymbol{I}_{\boldsymbol{k}}(s) = \boldsymbol{Y}_{\boldsymbol{k}}(s)\boldsymbol{V}_{\boldsymbol{k}}(s) \end{aligned} \tag{1}$$

Manuscript received March 30, 2001; revised August 24, 2001.
The authors are with the Department of Electronics, Carleton University, Ottawa, ON, Canada K1S 5B6.
Publisher Item Identifier S 0018-9480(01)10466-7.

where

- $\boldsymbol{x}_{\phi}(t)$ is a vector, which include node voltages appended by independent and dependent voltage source currents, inductor currents, nonlinear capacitor charge, and nonlinear inductor flux waveform. $\boldsymbol{G}_{\phi}$ and $\boldsymbol{C}_{\phi}$ are constant matrices describing the lumped memoryless and memory elements of the network, respectively. $\boldsymbol{b}_{\phi}(t)$ is a vector with entries determined by the independent voltage and current sources. $\boldsymbol{f}_{\phi}(\boldsymbol{x}_{\phi}(t))$ is a vector describing the nonlinear elements.
- $\boldsymbol{D_k} = [d_{i,j} \in \{0, 1\}]$ is a selector matrix that maps $\boldsymbol{i_k}(t)$, the vector of terminal currents entering the interconnect subnetwork k, into the node space of the network, where $i \in \{1, \ldots, n\}, j \in \{1, \ldots, 2m_k\}$ and m_k is the number of coupled signal conductors in subnetwork k. N_t is the number of distributed structures. $\boldsymbol{Y_k}(s)$ is the admittance parameters of interconnect subnetwork k in the Laplace domain. $\boldsymbol{I_k}$ and $\boldsymbol{V_k}$ represent the Laplace terminal voltages and currents of interconnect k.

The distributed elements in (1) do not have a direct representation in the time domain, leading to mixed frequency/time simulation difficulty. In order to overcome this problem, a closed-form MTL model based on a Padé matrix-rational approximation has recently been proposed [14]–[16]. This interconnect model is shown to be efficient, passive, and suitable for passive model reduction techniques based on congruent transformations. Using this *interconnect macromodel,* (1) can be expressed as

$$\boldsymbol{C}_{\pi} \frac{d}{dt} \boldsymbol{x}(t) + \boldsymbol{G}_{\pi}\boldsymbol{x}(t) + \boldsymbol{f}(\boldsymbol{x}(t)) = \boldsymbol{b}(t) \tag{2}$$

where the distributed elements are now explicitly embedded in the modified nodal admittance (MNA) [18] matrices of the overall network. The matrices of (2) are described in greater detail in Section IV, which describes the matrix-rational approximation-based algorithm.

III. Sensitivity Analysis

In this section, the sensitivity analysis is derived for both linear and nonlinear distributed networks.

A. Sensitivity Analysis of Linear Circuits

If distributed networks are not in the presence of nonlinear elements, then (2) can be expressed in the frequency domain as

$$(s\boldsymbol{C}_{\pi} + \boldsymbol{G}_{\pi})\boldsymbol{X} = \boldsymbol{B} \tag{3}$$

where $\boldsymbol{X}$ is the Laplace transform of $\boldsymbol{x}(t)$ and $\boldsymbol{B}$ is the Laplace transform of $\boldsymbol{b}(t)$. An efficient method to obtain the sensitivities of the network is the adjoint technique [18], [19]. Let Φ be the output variable of interest, defined as

$$\Phi = \boldsymbol{z^t X} \tag{4}$$

where $\boldsymbol{z}$ is a selector vector with unity entry corresponding to the output variable and the superscript t denotes the transpose of a matrix. Differentiating (3) and (4) with respect to a circuit parameter λ and combining the two relations yields

$$\frac{\partial \Phi}{\partial \lambda} = -\boldsymbol{X}_a^t \left(s \frac{\partial \boldsymbol{C}_{\pi}}{\partial \lambda} + \frac{\partial \boldsymbol{G}_{\pi}}{\partial \lambda} \right) \boldsymbol{X} \tag{5}$$

where $\boldsymbol{X}_a$ is the solution of the adjoint network and is defined as

$$(s\boldsymbol{C}_{\pi} + \boldsymbol{G}_{\pi})^t \boldsymbol{X}_a = \boldsymbol{z}. \tag{6}$$

From (5), the sensitivity of an output variable with respect to a circuit parameter depends on $\boldsymbol{X}$, $\boldsymbol{X}_a$, $\partial \boldsymbol{C}_{\pi}/\partial\lambda$, and $\partial \boldsymbol{G}_{\pi}/\partial\lambda$. The values of $\boldsymbol{X}$ and $\boldsymbol{X}_a$ are obtained from the solution of the network and adjoint equations given by (3) and (6), respectively. For the case where λ is an interconnect parameter, the matrices $\partial \boldsymbol{C}_{\pi}/\partial\lambda$ and $\partial \boldsymbol{G}_{\pi}/\partial\lambda$ are derived from the equations of the interconnect model. How to obtain these matrices from the matrix-rational approximation-based algorithm is described in Section IV.

B. Sensitivity Analysis With Nonlinear Terminations

The sensitivity of the nonlinear network with respect to a circuit parameter λ is obtained by differentiating (2) with λ as

$$\boldsymbol{C}_{\pi} \frac{d}{dt} \boldsymbol{z}(t) + \left(\boldsymbol{G}_{\pi} + \frac{\partial \boldsymbol{f}(\boldsymbol{x}(t))}{\partial \boldsymbol{x}(t)} \right) \boldsymbol{z}(t) + \boldsymbol{E}(t) = \boldsymbol{0} \tag{7}$$

where

$$\begin{aligned} \boldsymbol{E}(t) &= \frac{\partial \boldsymbol{C}_{\pi}}{\partial \lambda} \frac{d}{dt} \boldsymbol{x}(t) + \frac{\partial \boldsymbol{G}_{\pi}}{\partial \lambda} \boldsymbol{x}(t) + \frac{\partial \boldsymbol{f}(\boldsymbol{x}(t))}{\partial \lambda} \\ \boldsymbol{z} &= \frac{\partial \boldsymbol{x}(t)}{\partial \lambda}. \end{aligned} \tag{8}$$

The solution of (2) and (7) can be obtained by converting them to difference equations using integration formulae such as backward Euler or trapezoidal rule (TR) [18]. For example, if TR is used, (2) and (7) become

$$\begin{aligned} &\boldsymbol{A}\boldsymbol{X_{n+1}} + \frac{\boldsymbol{f}(\boldsymbol{X_{n+1}})}{2} \\ &\quad = \boldsymbol{B}\boldsymbol{X_n} - \frac{\boldsymbol{f}(\boldsymbol{X_n})}{2} + \frac{(\boldsymbol{b_{n+1}} + \boldsymbol{b_n})}{2} \end{aligned} \tag{9}$$

$$\begin{aligned} &\left(\boldsymbol{A} + \frac{\partial \boldsymbol{f}(\boldsymbol{X_{n+1}})}{2\partial \boldsymbol{X_{n+1}}} \right) \frac{\partial \boldsymbol{X_{n+1}}}{\partial \lambda} \\ &\quad = -\frac{\partial \boldsymbol{A}}{\partial \lambda} \boldsymbol{X_{n+1}} + \boldsymbol{B} \frac{\partial \boldsymbol{X_n}}{\partial \lambda} + \frac{\partial \boldsymbol{B}}{\partial \lambda} \boldsymbol{X_n} - \frac{\partial \boldsymbol{f}(\boldsymbol{X_n})}{2\partial \boldsymbol{X_n}} \frac{\partial \boldsymbol{X_n}}{\partial \lambda} \\ &\qquad - \frac{1}{2} \left(\frac{\partial f(\boldsymbol{X_{n+1}})}{\partial \lambda} + \frac{\partial f(\boldsymbol{X_n})}{\partial \lambda} \right) \end{aligned} \tag{10}$$

where

$$\boldsymbol{A} = \frac{\boldsymbol{C}_{\pi}}{\Delta t} + \frac{\boldsymbol{G}_{\pi}}{2} \qquad \boldsymbol{B} = \frac{\boldsymbol{C}_{\pi}}{\Delta t} - \frac{\boldsymbol{G}_{\pi}}{2} \tag{11}$$

and $\boldsymbol{X}_n = \boldsymbol{X}(t_n)$. The variable Δt is the time step between the time interval t_n to t_{n+1}.

Equations (9) and (10) represent the solution of the original and sensitivity networks as described by (2) and (7). The coefficients on the right side of (10) are all known from the solution of (9). The variables $\partial \boldsymbol{f}(\boldsymbol{X_{n+1}})/\partial \boldsymbol{X_{n+1}}$ and $\partial \boldsymbol{f}(\boldsymbol{X_n})/\partial \boldsymbol{X_n}$ are the Jacobean matrices which can be obtained by solving (9). The matrices $\partial \boldsymbol{A}/\partial\lambda$ and $\partial \boldsymbol{B}/\partial\lambda$ are derived from $\partial \boldsymbol{C}_{\pi}/\partial\lambda$ and $\partial \boldsymbol{G}_{\pi}/\partial\lambda$. For the case when λ is an interconnect parameter, $\partial \boldsymbol{C}_{\pi}/\partial\lambda$ and $\partial \boldsymbol{G}_{\pi}/\partial\lambda$ are derived from the equations of the interconnect model. How to obtain these matrices from the matrix-rational approximation-based algorithm will be described in Section IV.

C. Sensitivity With Respect to Physical Interconnect Parameters

When studying the sensitivity of distributed networks, the design parameters of interconnects are usually required with respect to physical parameters (such as width and spacing of conductors). The sensitivities of electrical parameters are often intermediate steps to the calculation of sensitivities of physical parameters. In the case where λ represents a physical parameter of an interconnect, the sensitivity of the output nodes can be obtained as follows:

$$\frac{\partial \boldsymbol{x}}{\partial \lambda} = \sum_{i=1}^{m_k} \sum_{j=1}^{m_k} \left(\frac{\partial \boldsymbol{x}}{\partial R_{i,j}} \frac{\partial R_{i,j}}{\partial \lambda} + \frac{\partial \boldsymbol{x}}{\partial L_{i,j}} \frac{\partial L_{i,j}}{\partial \lambda} + \frac{\partial \boldsymbol{x}}{\partial G_{i,j}} \frac{\partial G_{i,j}}{\partial \lambda} + \frac{\partial \boldsymbol{x}}{\partial C_{i,j}} \frac{\partial C_{i,j}}{\partial \lambda} \right) \quad (12)$$

where $R_{i,j}$, $L_{i,j}$, $G_{i,j}$, and $C_{i,j}$ are the per-unit-length parameters. The subscripts i and j are matrix indexes.

IV. Sensitivity of the Closed-Form Matrix-Rational Approximation-Based Macromodel

It is clear from Section III, to calculate network sensitivities with respect to any interconnect parameter, the MNA derivatives with respect to the interconnect parameters are required. This section reviews the closed-form matrix-rational approximation-based MTL macromodel, which forms the basis of the proposed algorithm. From this discussion, the MNA derivatives with respect to the interconnect parameters (i.e., $\partial \boldsymbol{C}_\pi / \partial \lambda$ and $\partial \boldsymbol{G}_\pi / \partial \lambda$) are derived.

A. Review of the Closed-Form Matrix-Rational Approximation-Based Macromodel

Consider a $m+1$ conductor transmission line (m signal conductors with one reference line) described by Telegrapher's equations

$$\frac{\partial}{\partial x} \boldsymbol{v}(x, t) = -\boldsymbol{R} \boldsymbol{i}(x, t) - \boldsymbol{L} \frac{\partial}{\partial t} \boldsymbol{i}(x, t)$$
$$\frac{\partial}{\partial x} \boldsymbol{i}(x, t) = -\boldsymbol{G} \boldsymbol{v}(x, t) - \boldsymbol{C} \frac{\partial}{\partial t} \boldsymbol{v}(x, t) \quad (13)$$

where $\boldsymbol{R}$, $\boldsymbol{L}$, $\boldsymbol{C}$, and $\boldsymbol{G} \in \Re^{m \times m}$ are the per-unit-length parameter matrices. The coefficients $\boldsymbol{v}(x, t)$ and $\boldsymbol{i}(x, t) \in \Re^m$ represent the voltage and current vectors, as a function of position x and time t. Equation (13) can be written in the Laplace domain using the exponential function as

$$\begin{bmatrix} \boldsymbol{V}(d, s) \\ \boldsymbol{I}(d, s) \end{bmatrix} = e^{\boldsymbol{Z}} \begin{bmatrix} \boldsymbol{V}(0, s) \\ \boldsymbol{I}(0, s) \end{bmatrix} \quad (14)$$

where

$$\boldsymbol{Z} = \begin{bmatrix} \boldsymbol{0} & -\boldsymbol{a}(s) \\ -\boldsymbol{b}(s) & \boldsymbol{0} \end{bmatrix} d; \;\; \boldsymbol{a}(s) = \boldsymbol{R} + s\boldsymbol{L}; \;\; \boldsymbol{b}(s) = \boldsymbol{G} + s\boldsymbol{C} \quad (15)$$

and d is the length of the line. The exponential matrix $e^{\boldsymbol{Z}}$ can be written as

$$e^{\boldsymbol{Z}} \approx [\boldsymbol{P}_N(\boldsymbol{Z})]^{-1} \boldsymbol{Q}_N(\boldsymbol{Z}) \quad (16)$$

where $\boldsymbol{P}_N(\boldsymbol{Z})$ and $\boldsymbol{Q}_N(\boldsymbol{Z})$ are ***polynomial matrices*** that can be expressed in terms of a closed-form matrix-rational function [14], [15]. Once $e^{\boldsymbol{Z}}$ is expressed as a rational function, it can be converted to ordinary differential equations. One way to obtain the differential equations is to express (16) in terms of subsections formed by the poles and zeros of the rational approximation. In this form, the macromodel can be represented in terms of lumped components [15].

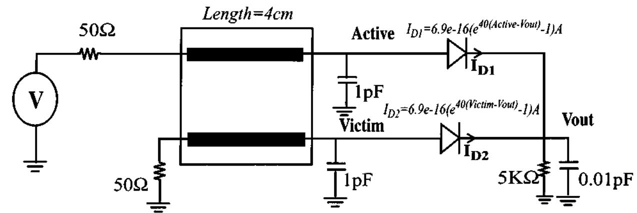

Fig. 1. Coupled interconnect system with nonlinear termination.

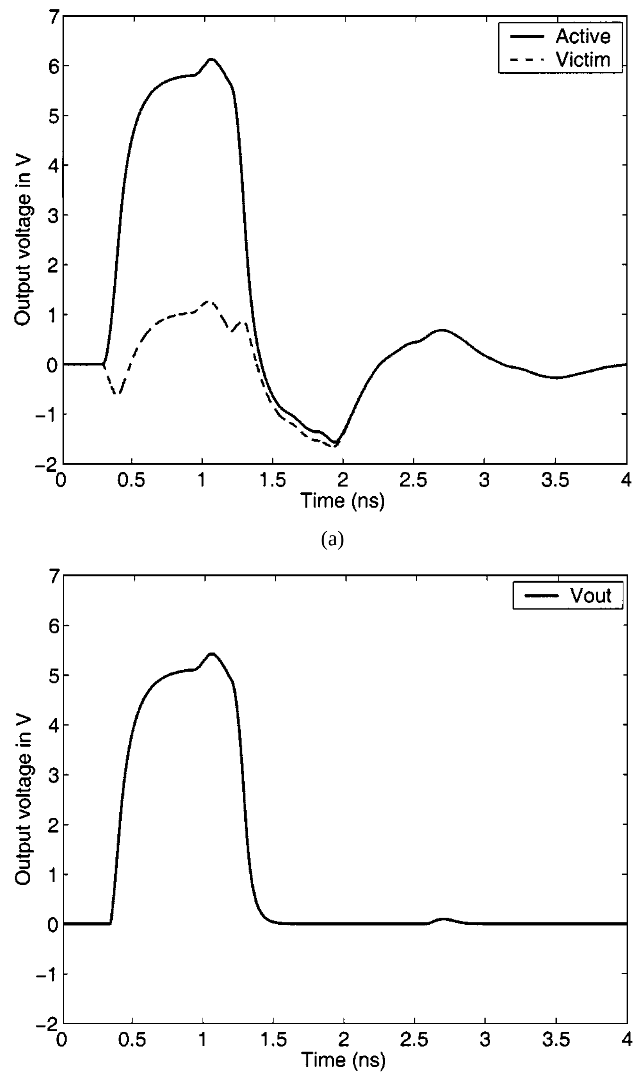

(a)

(b)

Fig. 2. Output transient of nonlinear circuit. (a) Response of active and victim line. (b) Response of $Vout$.

Using the proposed macromodel, the nonlinear distributed network described by (1) is converted into the form of (2) where

$$\boldsymbol{G}_\pi = \boldsymbol{G}_{\boldsymbol{a}} + \sum_{k=1}^{N_t} \sum_{i} (\psi_{\boldsymbol{i}}^{\boldsymbol{k}})^{\mathrm{t}} \boldsymbol{G}_{\boldsymbol{i}}^{\boldsymbol{k}} \psi_{\boldsymbol{i}}^{\boldsymbol{k}}$$
$$\boldsymbol{C}_\pi = \boldsymbol{C}_{\boldsymbol{a}} + \sum_{k=1}^{N_t} \sum_{i} (\psi_{\boldsymbol{i}}^{\boldsymbol{k}})^{\mathrm{t}} \boldsymbol{C}_{\boldsymbol{i}}^{\boldsymbol{k}} \psi_{\boldsymbol{i}}^{\boldsymbol{k}}. \quad (17)$$

Here the matrices $\boldsymbol{G_a}$, $\boldsymbol{C_a}$, $\boldsymbol{f}(\boldsymbol{x}(t))$, and $\boldsymbol{b}(t)$ are obtained from $\boldsymbol{G}_\phi$, $\boldsymbol{C}_\phi$, $\boldsymbol{f}_\phi(\boldsymbol{x}_\phi(t))$, and $\boldsymbol{b}_\phi(t)$ by appending them by rows (and/or) columns that contain zeros to account for the extra variables required for the stamp of the transmission line. Thus, $\boldsymbol{G_a}$, $\boldsymbol{C_a}$, $\boldsymbol{b}(t)$, and $\boldsymbol{f}(\boldsymbol{x}(t))$ can be expressed in the following block form:

$$\boldsymbol{G_a} = \begin{bmatrix} \boldsymbol{G}_\phi & \boldsymbol{0} \\ \boldsymbol{0} & \boldsymbol{0} \end{bmatrix}$$
$$\boldsymbol{C_a} = \begin{bmatrix} \boldsymbol{C}_\phi & \boldsymbol{0} \\ \boldsymbol{0} & \boldsymbol{0} \end{bmatrix}$$
$$\boldsymbol{f}(\boldsymbol{x}(t)) = \begin{bmatrix} \boldsymbol{f}_\phi(\boldsymbol{x}_\phi(t)) \\ \boldsymbol{0} \end{bmatrix}$$
$$\boldsymbol{b}(t) = \begin{bmatrix} \boldsymbol{b}_\phi(t) \\ \boldsymbol{0} \end{bmatrix}. \tag{18}$$

The indexes i and k represent the ith subsection of the kth interconnect. The subsections of each interconnect are obtained from the poles and zeros of the Padé rational model of the exponential function. In the case of real pole-zero subsections, they can be expressed as (19a) and (19b), shown at the bottom of this page. For the complex pole-zero subsections, the matrices are expressed as (20a) and (20b), shown at the bottom of the following page.

The matrices $\psi_{\boldsymbol{i}}^{\boldsymbol{k}}$ are selector matrices that map the block stamps $\boldsymbol{G_i^k}$ and $\boldsymbol{C_i^k}$ to the rest of the network equations. The matrices $\boldsymbol{R_k}$, $\boldsymbol{L_k}$, $\boldsymbol{C_k}$, and $\mathbf{G_k}$ are the per-unit-length parameters of the kth MTL, d_k is the length of the kth MTL, $\boldsymbol{U}$ is the unity matrix, and the variables $a_{i,k}$, $x_{i,k}$, and $\rho_{i,k}^2$ are predetermined constants given by the Padé approximation and are described in greater detail in [14] and [15].

It should be noted that the MNA matrices described by (19) and (20) are obtained analytically in terms of per-unit-length parameters and predetermined constants given by the matrix-rational approximation. An error criteria for selecting the order of the matrix-rational approximation is described in [14] and [15]. Next, the calculation of $\partial \boldsymbol{C}_\pi/\partial\lambda$ and $\partial \boldsymbol{G}_\pi/\partial\lambda$ is derived using the proposed MTL model.

B. Calculation of $\partial \boldsymbol{C}_\pi/\partial\lambda$ and $\partial \boldsymbol{G}_\pi/\partial\lambda$

To calculate the sensitivity of the network with respect to an interconnect parameter, the matrices $\partial \boldsymbol{C}_\pi/\partial\lambda$ and $\partial \boldsymbol{G}_\pi/\partial\lambda$ are required. The calculation of $\partial \boldsymbol{C}_\pi/\partial\lambda$ and $\partial \boldsymbol{G}_\pi/\partial\lambda$ depends on the interconnect model being used. For the case of matrix-rational approximation-based model, the matrices are obtained as follows. Let λ_k be an interconnect parameter of the kth interconnect. Differentiating the matrices of (17) with respect to λ_k yields

$$\frac{\partial \boldsymbol{G}_\pi}{\partial \lambda_k} = \sum_i (\psi_{\boldsymbol{i}}^{\boldsymbol{k}})^t \, \frac{\partial \boldsymbol{G_i^k}}{\partial \lambda_k} \, \psi_{\boldsymbol{i}}^{\boldsymbol{k}}$$
$$\frac{\partial \boldsymbol{C}_\pi}{\partial \lambda_k} = \sum_i (\psi_{\boldsymbol{i}}^{\boldsymbol{k}})^t \, \frac{\partial \boldsymbol{C_i^k}}{\partial \lambda_k} \, \psi_{\boldsymbol{i}}^{\boldsymbol{k}}. \tag{21}$$

The matrices $\partial \boldsymbol{C_i^k}/\partial\lambda_k$ and $\partial \boldsymbol{G_i^k}/\partial\lambda_k$ are computed analytically in terms of per-unit-length parameters and predetermined constants given by the matrix-rational approximation. This makes the formulation of sensitivity networks extremely simple when compared to other MTL models. As an example, differentiating with respect to the conductance of the kth interconnect for the complex pole-zero subsection yields $\partial \boldsymbol{C_i^k}/\partial G_k = \boldsymbol{0}$ and

$$\frac{\partial \boldsymbol{G_i^k}}{\partial G_k} = \begin{bmatrix} \frac{d_k}{4x_{i,k}} & 0 & 0 & \frac{-d_k}{4x_{i,k}} & 0 & 0 & 0 \\ 0 & 0 & 0 & 0 & 0 & 0 & 0 \\ 0 & 0 & \frac{x_{i,k} d_k}{\rho_{i,k}^2} & \frac{x_{i,k} d_k}{\rho_{i,k}^2} & 0 & 0 & 0 \\ \frac{-d_k}{4x_{i,k}} & 0 & \frac{x_{i,k} d_k}{\rho_{i,k}^2} & \left(\frac{x_{i,k} d_k}{\rho_{i,k}^2} + \frac{d_k}{4x_{i,k}}\right) & 0 & 0 & 0 \\ 0 & 0 & 0 & 0 & 0 & 0 & 0 \\ 0 & 0 & 0 & 0 & 0 & 0 & 0 \\ 0 & 0 & 0 & 0 & 0 & 0 & 0 \end{bmatrix} \tag{22}$$

for a single conductor line (with reference ground).

$$\boldsymbol{G}_i^k = \begin{bmatrix} \frac{d_k}{2a_{i,k}} \boldsymbol{G}_k & \boldsymbol{0} & \frac{d_k}{2a_{i,k}} \boldsymbol{G}_k & \boldsymbol{U} \\ \boldsymbol{0} & \frac{a_{i,k}}{2d_k} \boldsymbol{R}_k^{-1} & \frac{-a_{i,k}}{2d_k} \boldsymbol{R}_k^{-1} & -\boldsymbol{U} \\ \frac{d_k}{2a_{i,k}} \boldsymbol{G}_k & \frac{-a_{i,k}}{2d_k} \boldsymbol{R}_k^{-1} & \left(\frac{a_{i,k}}{2d_k} \boldsymbol{R}_k^{-1} + \frac{d_k}{2a_{i,k}} \boldsymbol{G}_k\right) & \boldsymbol{0} \\ -\boldsymbol{U} & \boldsymbol{U} & \boldsymbol{0} & \boldsymbol{0} \end{bmatrix} \tag{19a}$$

$$\boldsymbol{C}_i^k = \begin{bmatrix} \frac{d_k}{2a_{i,k}} \boldsymbol{C}_k & \boldsymbol{0} & \frac{d_k}{2a_{i,k}} \boldsymbol{C}_k & \boldsymbol{0} \\ \boldsymbol{0} & \boldsymbol{0} & \boldsymbol{0} & \boldsymbol{0} \\ \frac{d_k}{2a_{i,k}} \boldsymbol{C}_k & \boldsymbol{0} & \frac{d_k}{2a_{i,k}} \boldsymbol{C}_k & \boldsymbol{0} \\ \boldsymbol{0} & \boldsymbol{0} & \boldsymbol{0} & \frac{2d_k}{a_{i,k}} \boldsymbol{L}_k \end{bmatrix} \tag{19b}$$

V. Computation Results

Example 1: A coupled interconnect system with nonlinear termination is shown in Fig. 1. The length of the line is 4 cm and the per-unit-length parameters are

$$R = \begin{bmatrix} 0.14 & 0 \\ 0 & 0.14 \end{bmatrix} \Omega/\text{cm}$$

$$L = \begin{bmatrix} 6.3 & 2.9 \\ 2.9 & 6.3 \end{bmatrix} \text{nH/cm}$$

$$C = \begin{bmatrix} 1.1 & -0.45 \\ -0.45 & 1.1 \end{bmatrix} \text{pF/cm.}$$

Fig. 2 shows transient responses of the far-end voltages corresponding to a 5-V input pulse with rise/fall times 0.1 ns and a pulsewidth of 0.8 ns. The sensitivities with respect to C_{11} for the active, victim, and $V\text{out}$ nodes are shown in Fig. 3. The results of the proposed method are compared with the perturbation of the lumped segment model [8] (referred to as SPICE Perturbation). Both the proposed method and the perturbation results are in good agreement.

It is to be noted that using the proposed method provides the following advantages.

1) Using the closed-form matrix-rational approximation-based macromodel provides significant CPU advantages compared to the lumped segmentation model [15]. For this example, the total size of the MNA matrices was 93 × 93 using the proposed method while the size of the lumped model was 407 × 407.
2) Perturbation-based techniques can lead to inaccurate results (depending on the magnitude of the perturbation).
3) In addition, the nonlinear differential equations representing the perturbed network must be solved separately for every parameter of interest. However, in the proposed approach, the sensitivity information with respect to all the parameters can be essentially obtained from the solution of the original network.

Table I shows a comparison of savings in the main computational cost (in terms of total number of LU decompositions) using the proposed approach versus the perturbation approach, for the above example.

Example 2: In this example, interconnect physical parameters are optimized to obtain desired circuit performance. A circuit with three interconnect subnetworks is shown in Fig. 4. Each subnetwork consists of two coupled transmission lines and a ground plane, as shown Fig. 5. A 5-V step response with a

$$\boldsymbol{G}_i^k = \begin{bmatrix} \left(\frac{x_{i,k}}{d_k} + \frac{\rho_{i,k}^2}{4x_{i,k}d_k}\right)\boldsymbol{R}_k^{-1} + \frac{d_k}{4x_{i,k}}\boldsymbol{G}_k & \frac{-x_{i,k}}{d_k}\boldsymbol{R}_k^{-1} & \mathbf{0} & \frac{-d_k}{4x_{i,k}}\boldsymbol{G}_k & \frac{-\rho_{i,k}^2}{4x_{i,k}d_k}\boldsymbol{R}_k^{-1} & \mathbf{0} & \mathbf{0} \\ \frac{-x_{i,k}}{d_k}\boldsymbol{R}_k^{-1} & \frac{x_{i,k}}{d_k}\boldsymbol{R}_k^{-1} & \mathbf{0} & \mathbf{0} & \mathbf{0} & \boldsymbol{U} & \mathbf{0} \\ \mathbf{0} & \mathbf{0} & \frac{x_{i,k}d_k}{\rho_{i,k}^2}\boldsymbol{G}_k & \frac{x_{i,k}d_k}{\rho_{i,k}^2}\boldsymbol{G}_k & \mathbf{0} & -\boldsymbol{U} & \mathbf{0} \\ \frac{-d_k}{4x_{i,k}}\boldsymbol{G}_k & \mathbf{0} & \frac{x_{i,k}d_k}{\rho_{i,k}^2}\boldsymbol{G}_k & \left(\frac{x_{i,k}d_k}{\rho_{i,k}^2} + \frac{d_k}{4x_{i,k}}\right)\boldsymbol{G}_k & \mathbf{0} & \mathbf{0} & \boldsymbol{U} \\ \frac{-\rho_{i,k}^2}{4x_{i,k}d_k}\boldsymbol{R}_k^{-1} & \mathbf{0} & \mathbf{0} & \mathbf{0} & \frac{\rho_{i,k}^2}{4x_i d_k}\boldsymbol{R}_k^{-1} & \mathbf{0} & -\boldsymbol{U} \\ \mathbf{0} & -\boldsymbol{U} & \boldsymbol{U} & \mathbf{0} & \mathbf{0} & \mathbf{0} & \mathbf{0} \\ \mathbf{0} & \mathbf{0} & \mathbf{0} & -\boldsymbol{U} & \boldsymbol{U} & \mathbf{0} & \mathbf{0} \end{bmatrix} \tag{20a}$$

$$\boldsymbol{C}_i^k = \begin{bmatrix} \frac{d_k}{4x_{i,k}}\boldsymbol{C}_k & \mathbf{0} & \mathbf{0} & \frac{-d_k}{4x_{i,k}}\boldsymbol{C}_k & \mathbf{0} & \mathbf{0} & \mathbf{0} \\ \mathbf{0} & \mathbf{0} & \mathbf{0} & \mathbf{0} & \mathbf{0} & \mathbf{0} & \mathbf{0} \\ \mathbf{0} & \mathbf{0} & \frac{x_{i,k}d_k}{\rho_{i,k}^2}\boldsymbol{C}_k & \frac{x_{i,k}d_k}{\rho_{i,k}^2}\boldsymbol{C}_k & \mathbf{0} & \mathbf{0} & \mathbf{0} \\ \frac{-d_k}{4x_{i,k}}\boldsymbol{C}_k & \mathbf{0} & \frac{x_{i,k}d_k}{\rho_{i,k}^2}\boldsymbol{C}_k & \left(\frac{x_{i,k}d_k}{\rho_{i,k}^2} + \frac{d_k}{4x_{i,k}}\right)\boldsymbol{C}_k & \mathbf{0} & \mathbf{0} & \mathbf{0} \\ \mathbf{0} & \mathbf{0} & \mathbf{0} & \mathbf{0} & \mathbf{0} & \mathbf{0} & \mathbf{0} \\ \mathbf{0} & \mathbf{0} & \mathbf{0} & \mathbf{0} & \mathbf{0} & \frac{d_k}{x_{i,k}}\boldsymbol{L}_k & \mathbf{0} \\ \mathbf{0} & \mathbf{0} & \mathbf{0} & \mathbf{0} & \mathbf{0} & \mathbf{0} & \frac{4x_{i,k}d_k}{\rho_{i,k}^2}\boldsymbol{L}_k \end{bmatrix} \tag{20b}$$

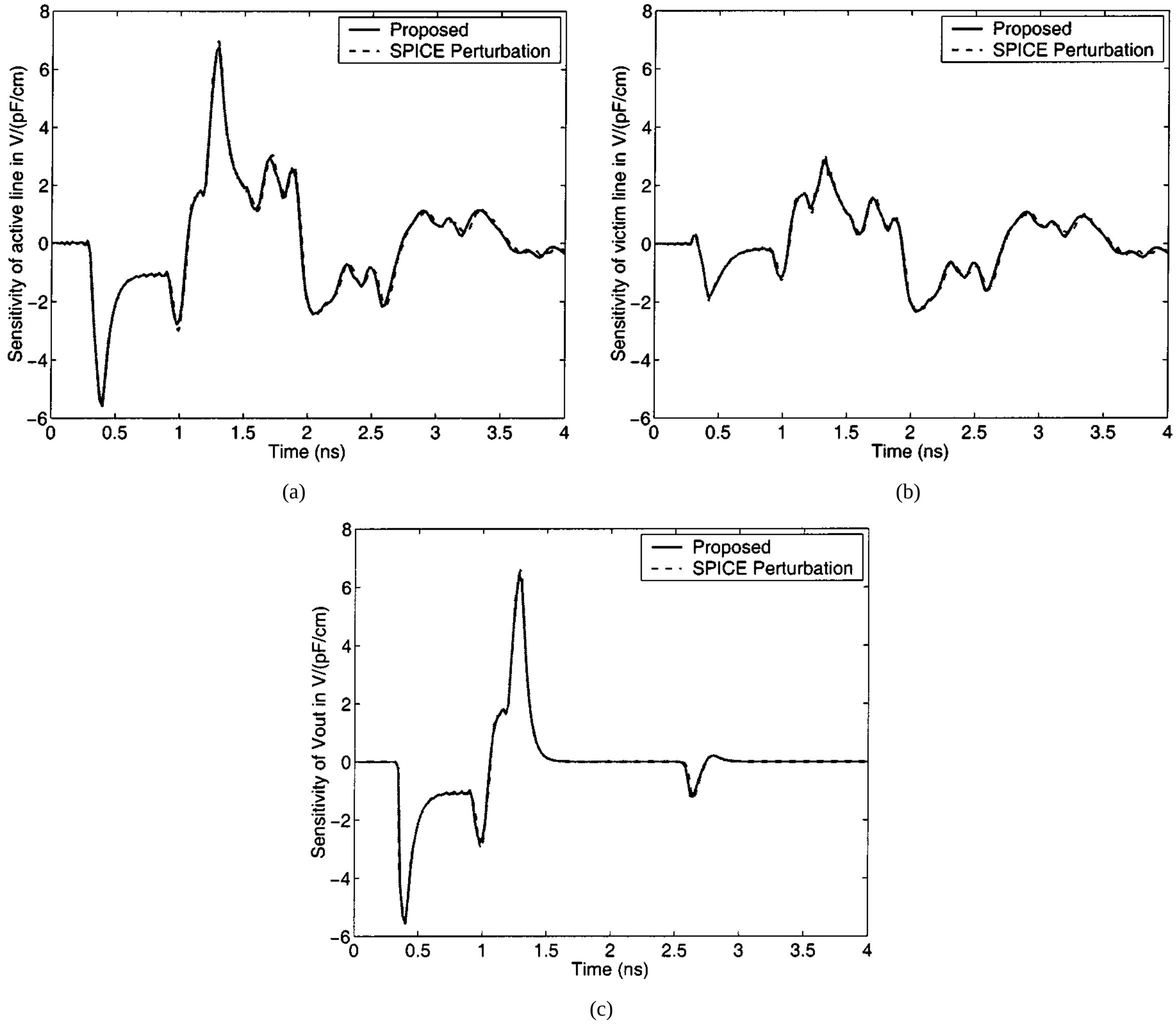

Fig. 3. Sensitivity w.r.t. C_{11} for: (a) the active line, (b) the victim line, and (c) $V\mathrm{out}$.

TABLE I
COMPUTATIONAL COMPLEXITY: PROPOSED VERSUS PERTURBATION

# of parameters	Perturbation (# LU decompositions)	Proposed (# LU decompositions)
10	17501	1601

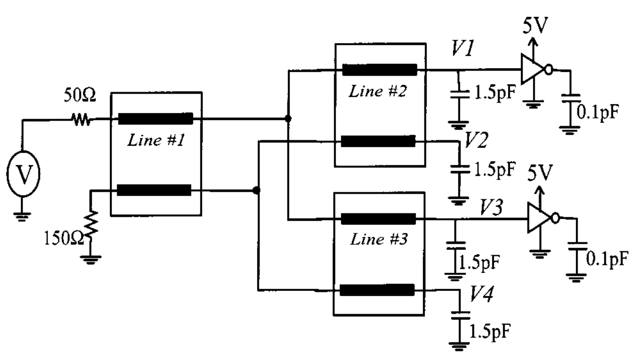

Fig. 4. Three coupled interconnects with nonlinear terminations.

time rise of 1 ns is the input signal of the circuit. The response of interest are nodes labeled V_1, V_2, V_3, and V_4. The responses before optimization are plotted in Fig. 6. The delays of V_1 and

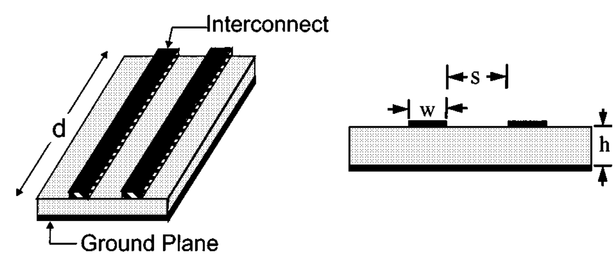

Fig. 5. Physical/geometrical parameters in a two-conductor transmission line.

V_3 are to be reduced to 5.5 and 5.0 ns, respectively, based on a threshold voltage of 3.0 V. In addition, it is desired to maintain the voltages of V_1 and V_3 greater then 4 V after 6.5 and 6.0 ns, respectively. A 0.4-V upper specification is imposed on the magnitude of V_2 and V_4. The error functions for V_1 and V_3 become

$$\begin{aligned}
e_1 &= \left[V_1(\phi,\, 5.5\ \mathrm{ns}) - 3\ \mathrm{V}\right]\\
e_2 &= -\left[V_1(\phi,\, 5.5\ \mathrm{ns}) - 3\ \mathrm{V}\right]\\
e_3 &= \left[V_3(\phi,\, 5.0\ \mathrm{ns}) - 3\ \mathrm{V}\right]\\
e_4 &= -\left[V_3(\phi,\, 5.0\ \mathrm{ns}) - 3\ \mathrm{V}\right]\\
e_{i+4} &= -\left[V_1(\phi,\, t_i) - 4\ \mathrm{V}\right]\\
e_{j+20} &= -\left[V_3(\phi,\, t_j) - 4\ \mathrm{V}\right]
\end{aligned}$$

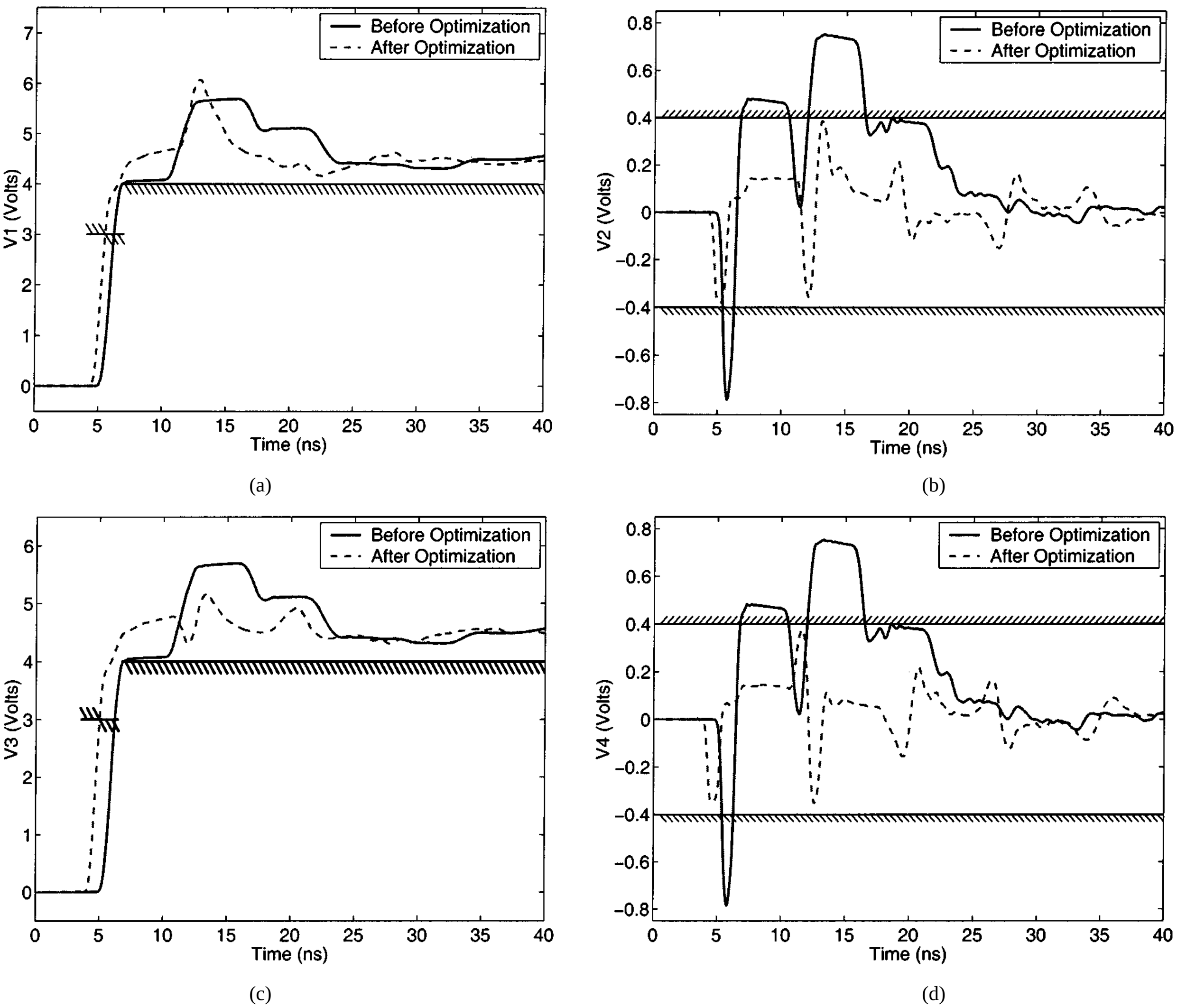

Fig. 6. Signal response of nonlinear circuit before and after optimization (example 3). (a) Signal response $V1$. (b) Sign response $V2$. (c) Signal response $V3$. (d) Signal response $V4$.

where $i = [1, 2, \ldots, 16]$, $j = [1, 2, \ldots, 16]$, t_i and t_j are equidistant time points between the interval [6.5 ns, 40.0 ns] and [6.0 ns, 40.0 ns], respectively. A weight factor of 10 is used to make the error functions of V_2 and V_4 comparable in scale to those of V_1 and V_3. The error functions e_{37} to e_{100} for V_2 and V_4 become

$$\begin{aligned} e_{k+36} &= 10\left[V_2(\phi, t_k) - 0.4 \text{ V}\right] \\ e_{k+52} &= -10\left[V_2(\phi, t_k) + 0.4 \text{ V}\right] \\ e_{k+68} &= 10\left[V_4(\phi, t_k) - 0.4 \text{ V}\right] \\ e_{k+84} &= -10\left[V_4(\phi, t_k) + 0.4 \text{ V}\right] \end{aligned}$$

where $k = [1, 2, \ldots, 16]$ and t_k are equidistant time points between the interval [0.0 ns, 40.0 ns]. As seen from Fig. 6, all specifications are violated before optimization.

The design variables ϕ include linewidth w, spacing between conductors s, circuit board thickness h, and lengths of multiconductor lines d_1, d_2, and d_3. Parameters w, s, and h are the same for all three transmission lines. Design constraints of the circuit require that the total length of the three transmission lines be 1.35 m and the total width of the two conductors plus the spacing between them be fixed at 2.5 mm. In addition, the width of the line has to be equal to or greater than 0.1 mm and the allowable range of the circuit board thickness is between 0.5–2.5 mm. The constraints on the design variables are

$$\begin{aligned} g_1(\phi) &= 2w + s - 2.5 \text{ mm} \\ g_2(\phi) &= d_1 + d_2 + d_3 - 1.35 \text{ m} \\ w &\geq 0.1 \text{ mm} \\ 0.5 \text{ mm} &\leq h \leq 2.5 \text{ mm}. \end{aligned}$$

The relative dielectric constants of the circuit board is 4.5. The initial values of the variables are $w = 0.5$ mm, $s = 1.5$ mm, $h = 2.0$ mm, $d1 = 0.45$ m, $d2 = 0.45$ m, and $d3 = 0.45$ m. The per-unit-length parameters are computed from the physical description of the transmission line by using an interconnect modeling tool [20]. The results obtained are used to formulate a lookup table. Intermediate data points are interpolated using Stirling's formula [21]. This results in relatively more accurate per-unit-length parameters during the optimization process.

The design variables after optimization are $w = 0.149$ mm, $s = 2.202$ mm, $h = 0.998$ mm, $d1 = 0.132$ m, $d2 = 0.651$ m, and $d3 = 0.567$ m. The optimized circuit responses are juxtaposed against those before optimization in Fig. 6. The new design variables meet all the circuit specifications without violating any design constraint.

VI. Conclusion

A new approach for sensitivity analysis of lossy multiconductor transmission lines in the presence of nonlinear terminations is described. Sensitivity information is derived from the recently developed closed-form matrix-rational approximation-based transmission-line model. The method enables sensitivity analysis of interconnect structures with respect to both electrical and physical parameters, while providing significant computational cost advantages.

References

[1] R. Sainati and T. Moravec, "Estimating high speed interconnect performance," *IEEE Trans. Circuits Syst.*, vol. 34, pp. 533–541, Apr. 1989.

[2] R. Achar and M. Nakhla, "Simulation of high-speed interconnects," *Proc. IEEE*, vol. 89, pp. 693–728, May 2001.

[3] M. Nakhla and R. Achar, "High-speed circuit and interconnect analysis I, and II," Omniz Global Knowledge Corporation, Ottawa, ON, Canada, [Online] Available: http://www.omniz.com, 2001.

[4] A. Deustsch, "Electrical characteristics of interconnections for high-performance systems," *Proc. IEEE*, vol. 86, pp. 315–355, Feb. 1998.

[5] Q. Zhang, S. Lum, and M. Nakhla, "Minimization of delay and crosstalk in high-speed VLSI interconnects," *IEEE Trans. Microwave Theory Tech.*, vol. 40, pp. 1555–1563, July 1992.

[6] S. Lum, M. Nakhla, and Q. Zhang, "Sensitivity analysis of lossy coupled transmission lines with nonlinear terminations," *IEEE Trans. Microwave Theory Tech.*, vol. 42, pp. 607–615, Apr. 1994.

[7] C. Jiao, A. C. Cangellaris, A. M. Yaghmour, and J. L. Prince, "Sensitivity analysis of multiconductor transmission lines and Optimization for high-speed interconnect circuit design," *IEEE Trans. Adv. Packag.*, vol. 23, pp. 132–141, May 2000.

[8] C. R. Paul, *Analysis of Multiconductor Transmission Line*. New York: Wiley, 1994.

[9] F. H. Branin, Jr., "Transient analysis of lossless transmission lines," *Proc. IEEE*, vol. 55, pp. 2012–2013, 1967.

[10] F. Y. Chang, "The generalized method of characteristics for wave-form relaxation analysis of coupled transmission lines," *IEEE Trans. Microwave Theory Tech.*, vol. 37, pp. 2028–2038, Dec. 1989.

[11] W. T. Beyene and J. E. Schutt-Ainé, "Accurate frequency-domain modeling and efficient simulation of high-speed packaging interconnects," *IEEE Trans. Microwave Theory Tech.*, vol. 45, pp. 1941–1947, Oct. 1997.

[12] O. A. Palusinski and A. Lee, "Analysis of transients in nonuniform and uniform multiconductor transmission lines," *IEEE Trans. Microwave Theory Tech.*, vol. 37, pp. 127–138, Jan. 1989.

[13] Q. Yu, J. M. L. Wang, and E. S. Kuh, "Passive multipoint moment matching model order reduction algorithm on multiport distributed interconnect networks," *IEEE Trans. Circuits Syst. I*, vol. 46, pp. 140–160, Jan. 1999.

[14] A. Dounavis, X. Li, M. Nakhla, and R. Achar, "Passive closed-loop transmission line model for general purpose circuit simulators," *IEEE Trans. Microwave Theory Tech.*, vol. 47, pp. 2450–2459, Dec. 1999.

[15] A. Dounavis, R. Achar, and M. Nakhla, "Efficient passive circuit models for distributed networks with frequency-dependent parameters," *IEEE Trans. Adv. Packag.*, pp. 382–392, Aug. 2000.

[16] A. Dounavis, E. Gad, R. Achar, and M. Nakhla, "Passive model reduction of multiport distributed interconnects," *IEEE Trans. Microwave Theory Tech.*, vol. 48, pp. 2325–2334, Dec. 2000.

[17] A. Odabasioglu, M. Celik, and L. T. Pilleggi, "PRIMA: Passive reduced-order interconnect macromodeling algorithm," *IEEE Trans. Computer-Aided Design*, vol. 17, pp. 645–653, Aug. 1998.

[18] J. Vlach and K. Singhal, *Computer Methods for Circuit Analysis and Design*. New York: Van Nostrand, 1983.

[19] M. Mongiardo and R. Ravenelli, "Automated design of corrugated feeds by adjoint network method," *IEEE Trans. Microwave Theory Tech.*, vol. 45, pp. 787–793, May 1997.

[20] *LINPAR Version 1.2*, Artech House, Norwood, MA, 1989.

[21] F. B. Hildebrand, *Introduction to Numerical Analysis*. New York: Dover, 1987.

Anestis Dounavis received the B.Eng. degree from McGill University, Montreal, QC, Canada, in 1995, the M.Eng. degree from Carleton University, Ottawa, ON, Canada, in 2000, and is currently working toward the Ph.D. degree in electronics at Carleton University.

His research interests include computer-aided design of very large scale integration (VLSI) systems, high-frequency interconnects, and numerical algorithms.

Mr. Dounavis was the recipient of the Carleton University Medal for his Master's thesis on time-domain macromodeling of high-speed interconnects.

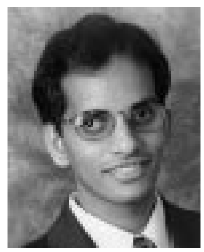

Ramachandra Achar (S'95–M'99) received the B.Eng. degree in electronics engineering from Bangalore University, Bangalore, India, in 1990, the M.Eng. degree in microelectronics from the Birla Institute of Technology and Science, Pilani, India, in 1992, and the Ph.D. degree from Carleton University, Ottawa, ON, Canada, in 1998.,

He is currently an Assistant Professor in the Department of Electronics, Carleton University. He spent the summer of 1995 involved with the macromodel development for high-speed linear circuits at the T. J. Watson Research Center, IBM. He was a graduate trainee at the Central Electronics Engineering Research Institute, Pilani, India, during 1992, and was also previously with Larsen and Toubro Engineers Ltd., Mysore, India, and with the Indian Institute of Science, Bangalore, India, as a Research and Development Engineer. From 1998 to 2000, he was a Research Engineer with the Computer-Aided Engineering (CAE) Group at Carleton University. His research interests include modeling and simulation of high-speed interconnects, numerical algorithms, and development of computer-aided design tools for high-frequency circuit analysis.

Dr. Achar was the recipient of the University Medal for his doctoral work on high-speed VLSI interconnect analysis while at Carleton University. He was also the recipient of several prestigious awards, including the Natural Science and Engineering Research Council (NSERC) Doctoral Award (2000), the Strategic Microelectronics Corporation (SMC) Award (1997), the Canadian Microelectronics Corporation (CMC) Award (1996), and the Best Student Paper Award at the 1998 Micronet (a Canadian network of centers of excellence on Microelectronics) Annual Workshop.

Michel S. Nakhla (S'73–M'75–SM'88–F'98) received the M.A.Sc. and Ph.D. degrees in electrical engineering from University of Waterloo, Waterloo, ON, Canada, in 1973 and 1975, respectively.

He is currently a Professor of electrical engineering at Carleton University, Ottawa, ON, Canada. From 1976 to 1988, he was with Bell-Northern Research, Ottawa, ON, Canada, as the Senior Manager of the Computer-Aided Engineering Group. In 1988, he joined Carleton University as a Professor and the Holder of the Computer-Aided Engineering Senior Industrial Chair established by Nortel Networks and the Natural Sciences and Engineering Research Council of Canada. He is the founder of the High-Speed Computer-Aided Design (CAD) Research Group, Carleton University, and is a frequent invited speaker on the topic of high-speed interconnects. He serves as technical consultant for several industrial organizations and is the principal investigator for several major sponsored research projects. His research interests include CAD of VLSI and microwave circuits, modeling and simulation of high-speed interconnects, nonlinear circuits, multidisciplinary optimization, thermal and electromagnetic (EM) emission analysis, microelectromechanical systems (MEMS), and neural networks.